ГИАБ. Горный информационно-аналитический бюллетень /
MIAB. Mining Informational and Analytical Bulletin, 2022;(10-2):5—23
ОРИГИНАЛЬНАЯ СТАТЬЯ / ORIGINAL PAPER

УДК 622 DOI: 10.25018/0236_1493_2022_102_0_5

АВТОМАТИЗАЦИЯ СБОРА ДАННЫХ С ОДНОСТОРОННЕГО ТРЕХОСНОГО ПЕРМЕАМЕТРА С ИСПОЛЬЗОВАНИЕМ ДАТЧИКОВ ARDUINO

М. Физонга[1,2], Ю.Денг[1], Ф. Вонг[1], Е.К. Чикутве Чанда[2], В. Мутамбо[2], Б. Бунда[2], Е. Корир[3], Д. Бваля[4], Дж. Лиюнгу[5], П. Чипола[6]

[1] Институт геотехнической инженерии, Школа транспортной инженерии, Юго-Восточный университет, Нанкин, Китай;
[2] Горная школа Замбийского университета, Кампус Грейт-Ист-Роуд, Лусака, Замбия;
[3] Belgravia Services Limited;
[4] Отдел исследований и разработок Simples Energia Lda Rua Aleixo da mota 86, R / C 4150–044 Порту, Португалия;
[5] Инженерная школа Замбийского университета, Кампус Грейт-Ист-Роуд, Лусака, Замбия;
[6] FQM Trident limited, Калумбила, Северо-Запад, Замбия

Аннотация: определение и интерпретация гидравлической проводимости представляет собой сложный процесс в пористой среде. Точное измерение гидравлической проводимости требует лабораторных испытаний, мониторинга и прогнозирования. Это исследование направлено на изготовление одностороннего трехосного пермеаметра с гибкой стенкой для непрерывного мониторинга проницаемости и прогнозирования гидравлической проводимости с использованием машинного обучения. Изготовленное устройство оснащено датчиками Arduino в режиме реального времени для регистрации влажности, обратного давления, массы сточной воды, комнатной температуры и температуры сточной воды. При проектировании электрической схемы конденсатор и катушка индуктивности были взяты из поврежденного электронного устройства и использовались для подавления шума при колебаниях напряжения в цепи. Модель искусственной нейронной сети в R использовалась для прогнозирования массы статической нагрузки в 50 г, динамической нагрузки просачивающейся воды и коэффициента проницаемости. Стандартное отклонение приложенной статической нагрузки в течение 24 часов с помощью регрессионного анализа с первого по пятый день составило 1,08, 1,99, 1,68, 0,99 и 0,75 соответственно. Объединенные 5-дневные данные показали отклонение в 4,4, стандартное отклонение в 2,1 и среднее значение массы 49,93 г. Прогнозируемый коэффициент гидравлической проводимости исследованных образцов цементного раствора с медными остатками, отвержденного в течение 31 дня, состоящего из 25%-ной дозы цемента, составил 1.73e-9 м/с с высоким коэффициентом детерминации R=0,97. Использование датчиков в реальном времени и машинного обучения может помочь точно определить гидравлическую проводимость.

Ключевые слова: датчики Arduino; Arduino Uno; трехосный пермеаметр гибкой стенки; микроконтроллер; коэффициент гидравлической проводимости; машинное обучение.

Для цитирования: *Физонга М., Денг Ю., Вонг Ф., Чикутве Чанда Е.К., Мутамбо В., Бунда Б., Корир Е., Бваля Д., Лиюнгу Дж., Чипола П.* Автоматизация сбора данных с одностороннего трехосного пермеаметра с использованием датчиков Arduino // Горный информационно-аналитический бюллетень. — 2022. — № 10-2. — С. 5—23. DOI: 10.25018/0236_1493_2022_102_0_5.

Automation of data acquisition from a one-way Triaxial Permeameter using Arduino sensors

M. Fisonga[1,2], Y. Deng[1], F. Wang[1], E.K. Chikutwe Chanda[2], V. Mutambo[2], B. Bunda[2], E. Korir[3], D. Bwalya[4], J. Liyungu[5], P. Chipola[6]

[1] Institute of Geotechnical Engineering, School of Transport Engineering, Southeast University, Nanjing, China
[2] School of Mines, University of Zambia, Great East Road Campus, Lusaka, Zambia;
[3] Belgravia Services Limited;
[4] R&D Dept Simples Energia Lda Rua Aleixo da mota 86, R/C 4150–044 Porto, Portugal;
[5] School of Engineering, University of Zambia, Great East Road Campus, Lusaka, Zambia;
[6] FQM Trident limited, Kalumbila, Northwestern, Zambia

Abstract: The determination and interpretation of hydraulic conductivity is an intricate process in porous medium. Accurate measurement of hydraulic conductivity requires laboratory testing, monitoring and prediction. This study focuses on the fabrication of a one-way triaxial permeameter with a flexible wall for continuous permeability monitoring and hydraulic conductivity prediction using machine learning. The fabricated apparatus is equipped with real-time Arduino sensors to record humidity, backpressure, the mass of effluent water, room temperature and effluent water temperature. In the electrical circuit design, the capacitor and inductor were taken from a damaged electronic apparatus and used to buffer noise when the voltage in the circuit fluctuates. An artificial neural network model in R was used to predict the mass of the static load of 50g, the dynamic load of seeped water, and the coefficient of permeability. The standard deviation of the applied static load over 24 hours by regression analysis from day one to day five were 1.08, 1.99, 1.68, 0.99 and 0.75, respectively. The combined 5-day data showed a variance of 4.4, a standard deviation of 2.1, and a mean mass value of 49.93g. The predicted coefficient of hydraulic conductivity of the investigated samples of copper tailing cement slurry cured for 31 days comprised of 25% cement dosage was 1.73e-9 m/s with a high coefficient of determination R=0.97. The use of real-time sensing and machine learning can help accurately determine hydraulic conductivity.

Key words: Arduino sensors; Arduino Uno; flexible wall triaxial permeameter; microcontroller; coefficient of hydraulic conductivity; machine learning.

For citation: Fisonga M., Deng Y., Wang F., Chikutwe Chanda E.K., Mutambo V., Bunda B., Korir E., Bwalya D., Liyungu J., Chipola P. Automation of data acquisition from a one-way Triaxial Permeameter using Arduino sensors. *MIAB. Mining Inf. Anal. Bull.* 2022;(10-2):5–23. [In Russ]. DOI: 10.25018/0236_1493_2022_102_0_5.

1 Introduction

A three-axis permeameter with a flexible wall can be used to investigate the hydraulic and chemical conductivity of compacted fine-grained soils, soil cement, and soil cement bentonite [1], [2]. The coefficient of permeability is of key importance for evaluating seepage losses, pore water pressure, quicksand conditions, contamination control, and design of dewatering, dams, and drainage systems. However, acquiring an automated triaxial permeability testing apparatus is costly because of the technology used for its fabrication. On the other hand, manual data logging from a triaxial permeameter is accompanied by a variety of human and environmental errors that can lead to erroneous hydraulic conductivity determination.

It is known that an incremental temperature change alters the water

properties, hence affecting the hydraulic conductivity of soils [3]. The influence of temperature on hydraulic conductivity is explained by the fact that it affects the water viscosity [4], [5]. The determination and interpretation of hydraulic conductivity is a complex process in a porous medium [6]. This is because the determination of hydraulic conductivity is strongly influenced by the degree of saturation, absorbed water, trapped air, impurities in effluent water, temperature and degree of packing of soil cement. However, monitoring the factors that influence hydraulic conductivity determination requires a number of sensors to be connected to the permeameter system. Sensors that can be attached to the permeameter system refer to liquid level, pressure, humidity and temperature, etc. The different ways of measuring liquid levels have been investigated by previous researchers [7]. Load cells are some of the sensors that are used to measure liquid level [7],[10]. However, the load cell sensor is known to have creeping characteristics [11], [12]. In 2001, Kopczynski and Ness investigated five factors that affect the accuracy of weighing systems [13]. In this study, the apparatus was fabricated by reinventing the wheels of the one-way triaxial permeameter described by Head [14] at a reasonable cost.

This study focuses on the automation of a one-way triaxial permeameter with a flexible wall for testing the hydraulic conductivity of soils, soil-cement and soil-cement bentonite. The objectives of this experimental study are to: (1) automate data acquisition from the permeameter, (2) investigate the effect of environmental factors on the load cell to measure seepage, (3) investigate the stability of the load cell to continuously measure fluid levels for 24 hours, and (4) predict the coefficient of hydraulic conductivity using an artificial neural network in R [15].

2 Materials and Methods

The components shown in Table 1 were used to fabricate the automated one-way triaxial permeameter. Although these components produced favourable results, other sources of components were also used, but they did not produce the desired results.

2.1 Mix design and sample preparation

Mixing compositions for three samples of copper tailing cement slurry (CTCS) were prepared using the Mindola copper tailing (CT) by implementing dosage Equation 1. Due to the complexity of homogeneous mixing of fine-grained particles [17], it is necessary to thoroughly mix the dry CT and cement prior to the addition of the required amount of moulding water. After that, further mixing was required to form a homogeneous paste. Mixing dry CT with the Ordinary Portland Cement 42.5 N (OPC 42.5N) helps to avoid the inconsistency in distribution of OPC 42.5 N in the CTCS matrix. In the developed mix, the content of CT, OPC 42.5 N and mixing water was 1383g, 25% and 500 ml, respectively. The CTCS samples used in this study were cylindrical with a diameter of 50 mm and a height of 100 mm. The required temperature of the mixing chamber and the fog room temperatures corresponded to the ASTM-C511−13 standard [16]. The samples were kept in the fog room for 31 days, after which the samples were subjected to permeability and stress-strain tests. The stress-strain condition was determined using a CBR-2 test apparatus using gear 3 at a speed of 1.27 mm/min.

$$\text{Material dosage } (\%) = \\ = \frac{\text{Material component (g)}}{\text{Base Copper tailing (g)}} \cdot 100\%, \qquad (1)$$

2.2 Workability of the copper tailing cement slurry

The workability of the samples used in this study was checked through the

Table 1

Components used to fabricate the automated one-way triaxial permeameter

Material	Quantity (U)	Material	Quantity (U)
Plastic washers	8	50 g load cell calibration load	1
One-wire DS18B20 Dallas temperature sensor	1	Arduino accessories	1
DHT22 temperature-humidity sensor	1	5 kg Load Cell	1
2000gx0.1 Mini Libra Accurate Digital Scale	1	AR-2000 Pressure regulators	5
SCM Pipe connectors	12	CASUN 1.0 MPa Pressure Gauge	2
1.6 MPa Water Filter Containers	2	ROSS 24 Litre Compressor	1
5 Litre calibrated container	1	G1/4" 5V 0–0.5MPa Pressure Transducer Sensor Oil Fuel	1
PU6 Plastic pipe connectors	11	50 mm Porous Stones	6
LSA-6 Plastic pipe connectors	10	50 mm diameter to 100mm height plastic moulds	3
Flowmeter connectors	3	Thermometer	1
PY4–6 Plastic pipe connectors	8	XH-W3002 Thermometer	1
6mm Q91SA PN6.4 metal connectors	10	Electrical box (Permeameter outer casing)	1
6mm plastic connectors	15	Triaxial cells	1
6mm PVC pipe	1	G1/4 Aluminum Alloy Pressure Regulating Valve Air Regulator ml	2
12 v 1A charger	1	Thread tape	3

implementation of a miniature slump, to maintain the recommended slump by previous researchers ranging between 100–200 mm [17], [1]. The slump test of the designed mix was 105 mm, which corresponds to the recommended slump [17], [1].

2.3 Hydraulic conductivity

The constant head method according to the ASTM-D5084 [19] was used to carry out the permeability test. Computation of the coefficient of permeability in this study was in line with the implementation of Equation 2 [14]. The permeation was carried out in the fabricated one-way flexible-wall triaxial permeameter. Fig. 1 is an illustration of a schematic seepage

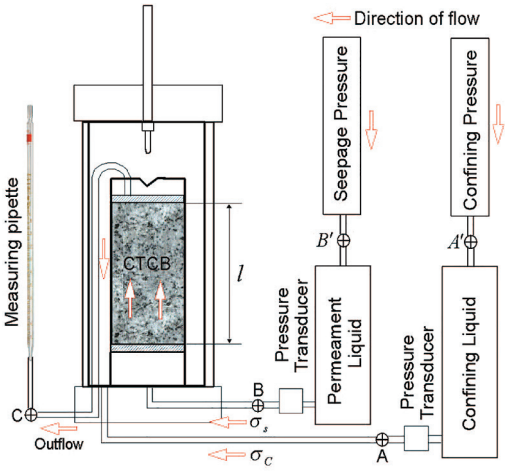

Fig. 1. Schematic diagram of the flexible-wall permeameter

permeability testing apparatus. After the required curing period for the three specimens, they were removed from the fog room, and thereafter the specimens were saturated until they reached a degree of saturation of >96%, followed by a permeability test. The determination of the coefficient of hydraulic conductivity was highly influenced by the applied confining and effective pressure [20].

$$k = \frac{ql}{\Delta hA}. \quad (2)$$

Where: q = discharge (m^3/s), k = coefficient of permeability (m/s), $i = \frac{\Delta h}{l}$ hydraulic gradient, l = thickness of the sample (m), $u = \Delta h \cdot \gamma_w$ pore water pressure (kPa) and A = area of sample (m^2). Unit weight of water of $\gamma_w = 9.81kN/m^3$, Δh = pressure head (m). The pore water pressure and confining pressure can be determined using Equation 3 and 4 respectively [14], [21]. Therefore, the top back pressure was considered to be null in the confining pressure determination.

$$u = \frac{1}{3}(2p_1 + p_2) \quad (3)$$

$$\sigma_C = \sigma_C{}' + u = \sigma_C{}' + \frac{1}{3}(2p_1 + p_2) \quad (4)$$

where: p_1 = top back pressure and p_2 = bottom back pressure

The one-way flexible-wall triaxial permeameter operates on a permeation seepage pressure basis. This is because the one-way flexible triaxial permeameter does not use the top backpressure. The seepage pressure can be calculated from the equation $\sigma_s = \Delta h \cdot \gamma_w$, where $\gamma_w = 9.81kN/m^3$ is the unit weight of water, Δh = Acting pressure head (m) [22]. Therefore, applying Equations 3 and 4 will result in the erroneous application of the required confining pressure. On the other hand, there is insufficient data in the literature on the determination of the required effective stress during the permeation using a one-way permeameter. However, due to the advantages offered by the Arduino data logging system, it is possible to investigate the determination of the required confinement and seepage pressures. The seepage pressure σ_S was kept constant at 134kPa to determine the required contact pressure and the rising differential pressure. Thereafter, the confining pressure was increased every hour, and the experiment lasted 8 hours 32 minutes, which allowed 60 records per hour to be recorded. The total number of records in the database was 511 records. However, the first record was deleted because the Arduino scale were placed on the tare at the beginning of the experiment. Therefore, the total number of records used in machine learning to determine the stability area was 510. The application of artificial neural networks (ANNs) in geotechnical engineering has been investigated by other researchers [23], [28]. However, in this study, an ANN was used to predict mass and hydraulic conductivity coefficient from the logged data. Through the use of the ANN, it was found that the stability region of the pressure drop was within 46–57%, which coincides with the logging dataset. A logistic model was fitted for the dependence of duration (seconds) on the coefficient of permeability and the percentage difference between the confining pressure and seepage pressure on the coefficient of permeability, as shown in Fig. 2. Applying a confining pressure greater than 57% resulted in a decrease in the coefficient of hydraulic conductivity. This phenomenon can be seen in Fig. 2, where the coefficient of permeability reached a steady state. Further increasing confining pressure resulted in a steady decrease in the coefficient of permeability. This could possibly be a result of the peripheral voids being clogged with the emulsion

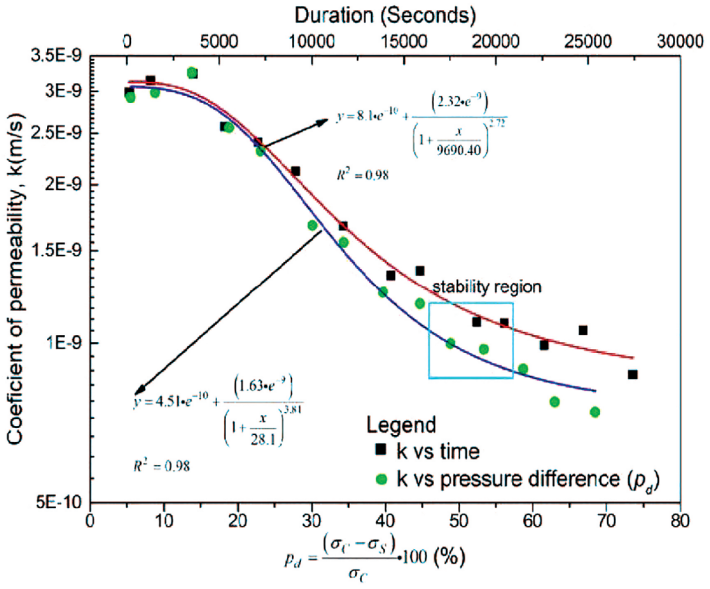

Fig. 2. Required stable confining pressure for the soil-cement sample

used to reduce the seepage of water between the contact of the CTCS sample and the rubber membrane. Taking into account the differential pressure stability region, Equation 5 can be used to determine the effective stress and Equation 6 can be used to determine the confining pressures.

$$\sigma'_C = p_d \cdot \sigma_s + \sigma_s \quad (5)$$

$$\sigma_C = \sigma'_C + \sigma_s \text{ or } \sigma_C = p_d \cdot \sigma_s + 2 \cdot \sigma_s \quad (6)$$

In this study, the acting water head was 11.7 m, resulting in the seepage pressure $\sigma_s = 115kPa$. Effective stress w $\sigma'_C = 181kPa$ and confining pressure $\sigma_C = 296kPa$ were used to execute the permeability testing. Fig. 3 shows the self-fabricated automated data logging flexible-wall triaxial permeameter.

2.4 Experimental procedures

The methodology used for this study is shown in Fig. 4. First, a one-way permeameter was designed. After the fabrication of the permeameter, the Arduino sensors were connected to

Fig. 3. Self-fabricated permeameter

the hardware. The connection of many Arduino sensors to the Arduino Uno is directly accompanied by voltage fluctuations. Therefore, in order to cut off the voltage fluctuations and noise in the designed circuit connection, it was necessary to introduce an electrolyte capacitor, some resistors, and an inductor, as shown in Fig. 5. The load cell was calibrated using a modified calibration code from Sparkfun [29]. The HX711 Arduino Library from Sparkfun was also

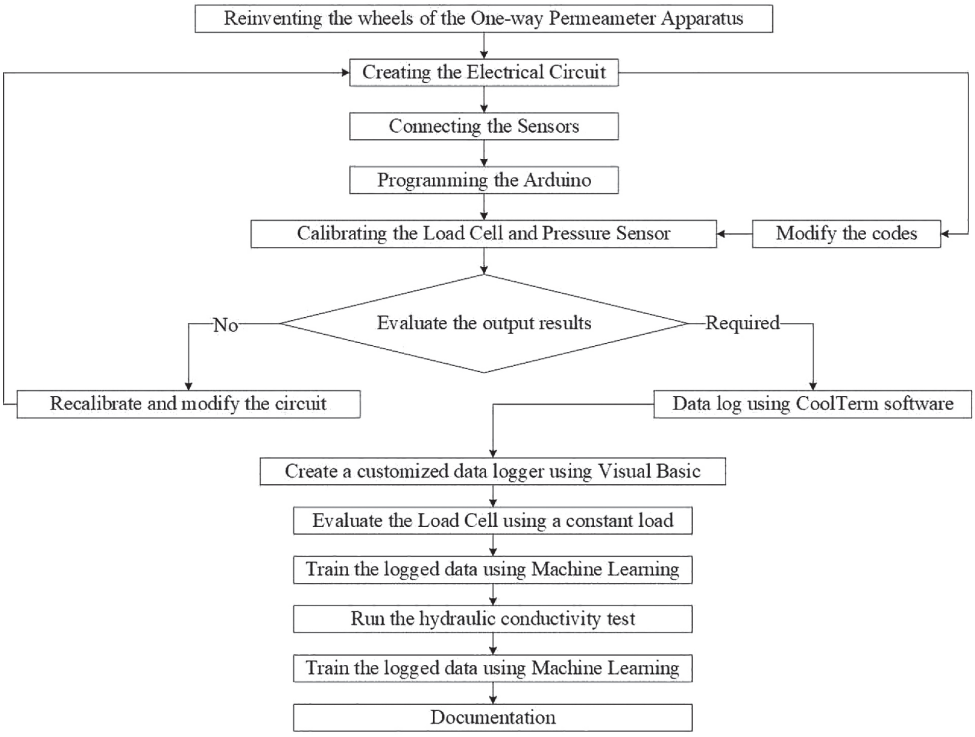

Fig. 4. Flow Chart of the research methodology

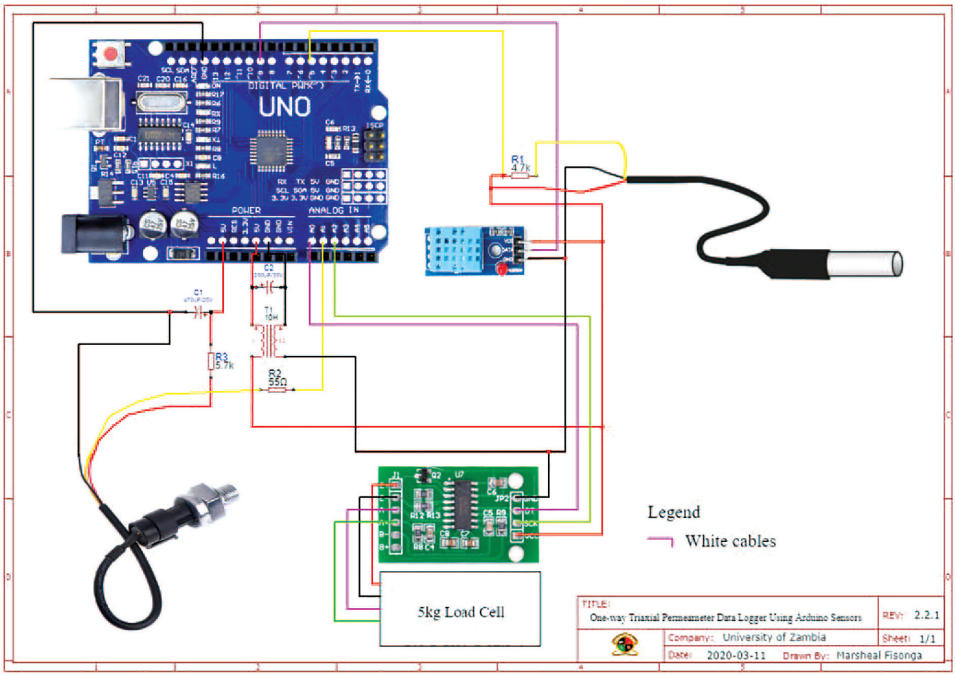

Fig. 5. One-Way Triaxial Permeameter Data Logger

used [29]. The programmed Arduino scale can accurately measure instantaneous loads from 1 gram to 5000 g.

3 Results and discussion

3.1 Datalogger

The automation of the data logging was done using Arduino sensors and an Arduino Uno microcontroller. After the sensors were connected, the data logger was programmed using the Arduino programming language, and the "OWTPReal Time Data Logger VS.2.2.1" software for individual data logging was programmed using Visual Basic Language, which is present in the integrated development environment Visual Studio [30]. The Arduino data logger and data logging software were programmed to read a signal every 60 seconds. The data logger can record the time in seconds (hours: minutes: seconds), date, current humidity, room temperature, water temperature, backpressure and the mass of seeped water. The temperature compensation code for the load cell was written in the Arduino code. Fig. 6 is the graphical user interface of the developed data logging application.

3.2 Load cell creeping

Other investigators have studied the load cell response to creep and recovery [11], [12], [31], [33]. In this study, a 50 g constant load was used to investigate the creep characteristics of the 5-kilogramArduino load cell at room temperature and humidity in real-time. It was found that the creep of the load cell is strongly influenced by temperature. This coincides with the documented results by Mohamed et al., which state that the creep of the load cell is strongly influenced by the thermoelastic effect [12]. Moreover, in this study, it was discovered that real-time humidity also has an effect on the creep of the load cell. The HK12-P138B 0.5 MPa pressure sensor was found to have no effect on the creep characteristics of the load cell as it was an independent sensor and was connected to a separate power supply from the Arduino Uno. The standard deviations of the mass from the regression analysis for days one, two, three, four, and five erewere 1.08, 1.99, 1.68, 0.99, and 0.75, respectively. Fig.s 7(A), (B), (C) and (D) show the regression analysis for time versus mass,

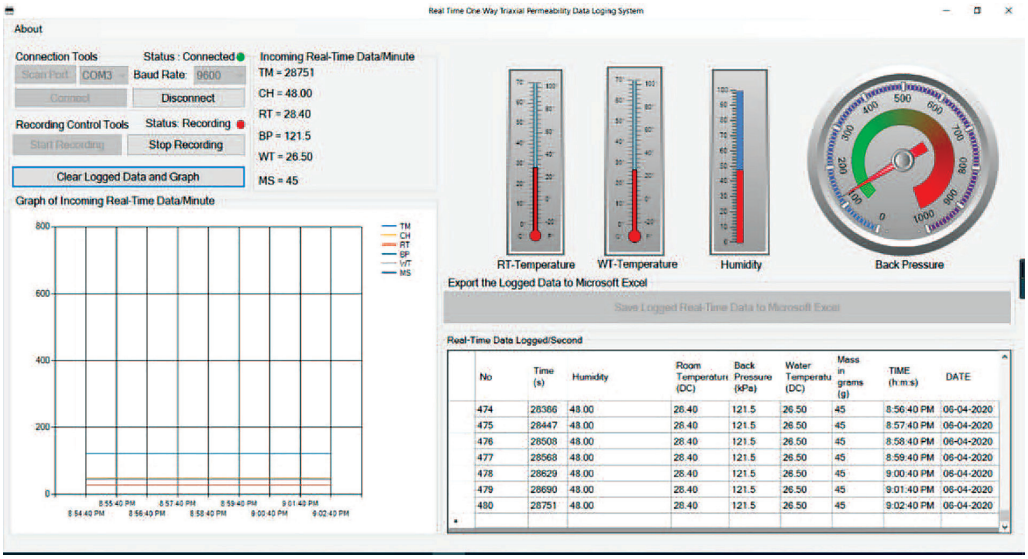

Fig. 6. The graphical user interface of the developed data logging application

time versus room temperature, time versus water temperature, and mass versus water temperatures for the first-day dataset. In addition, the variance of the first-day data set was 1.16 and the average mass was 51.77 g. Fig. 7 shows that temperature has a great effect on the creep characteristic of the load cell. Upon completion of the regression analysis for each day, the recorded data were combined to determine that the creep characteristic for the five days of the study had a variance of 4.4, a standard deviation of 2.1, and an average mass value of 49.93 g.

3.3 Constant load prediction

The load applied to the load cell as a result of the accumulation of the seepage water into the beaker can be considered as a dynamic load because of the nature of the application. Therefore, it became necessary to investigate the prediction of a 50 g constant load using ANN from the recorded data, where the two hidden layers were applied to each ANN model used in this study. However, to execute the ANN-based prediction, ANN prediction was first performed on individual datasets, and the results obtained are shown in Fig. 9. Fig. 9 shows that the change in constant load for the actual and predicted results for one day had a minimum and maximum value of 44.00 and 54.00, respectively. The five-day data was then combined and the ANN shown in Fig. 10 was implemented to predict the mass of the all-in-one dataset (AIOD), the results obtained with the AIOD are shown in Fig. 11. Fig.s 9 and 11 show that there is a strong linear relationship between the actual and the predicted values. For this reason, the ANN can help to predict mass for large data from the Arduino logged datasets. The AIOD prediction results in Fig. 11 showed a lower coefficient of determination than the individual dataset prediction results in Fig. 8. A root mean

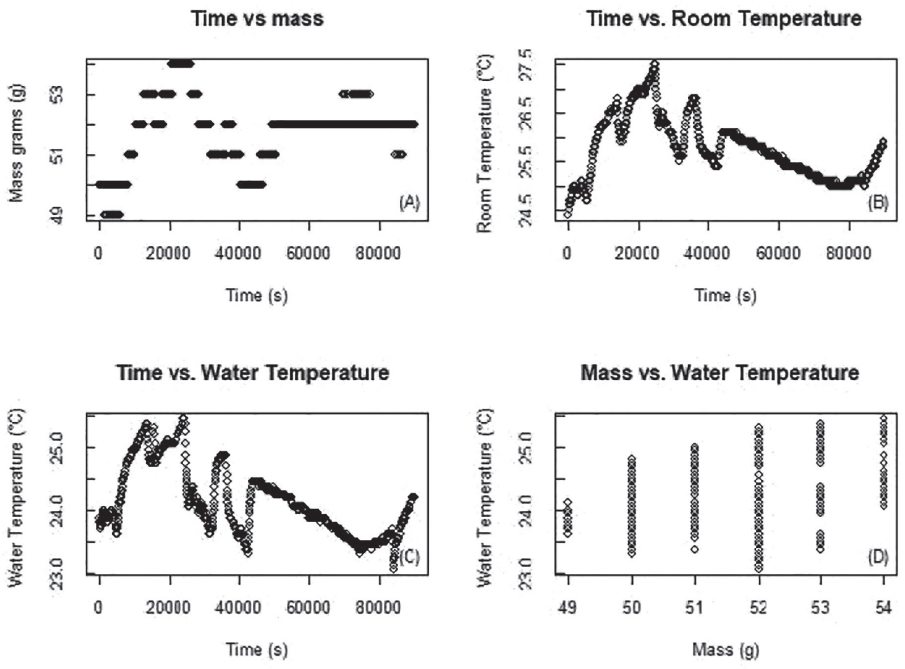

Fig. 7. Load cell creeping in relation to the temperature variations

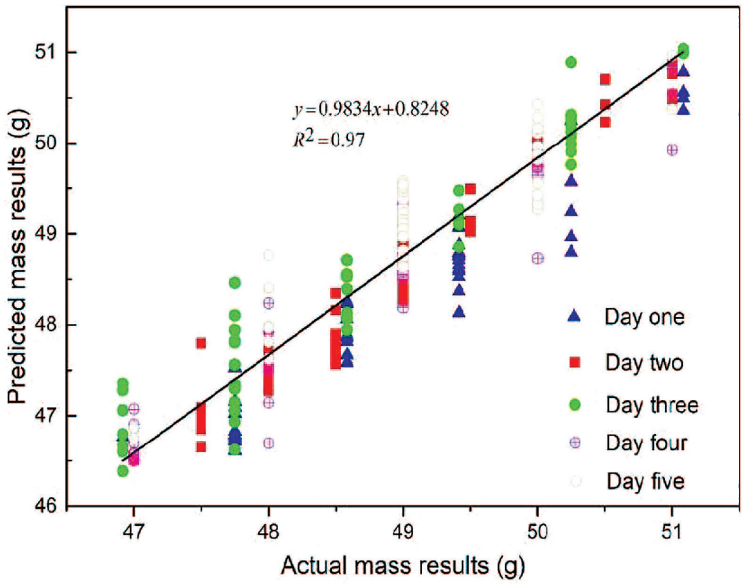

Fig. 8. Relationship between actual and predicted results

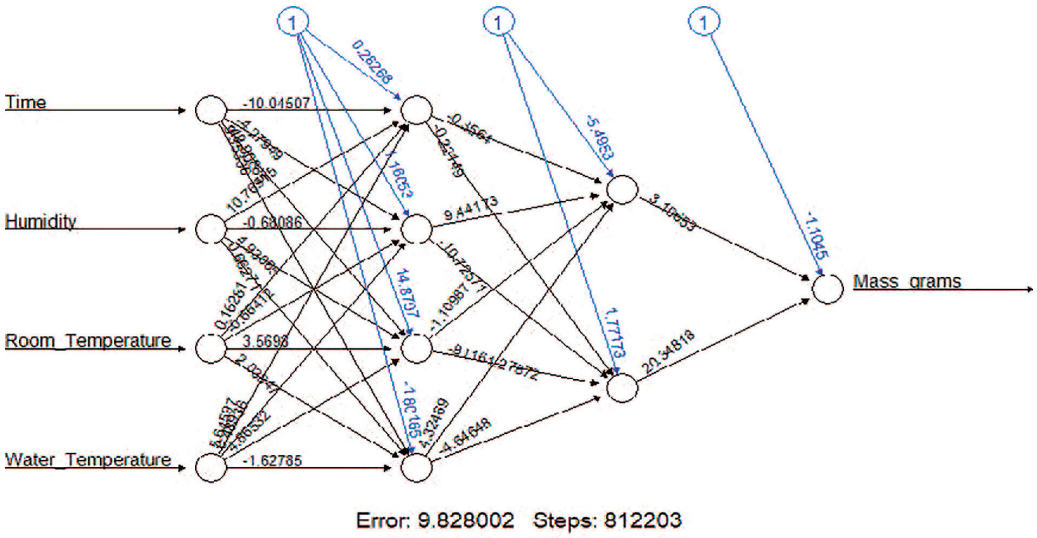

Fig. 9. Artificial Neural Network for AIOD

square error (RMSE) of 0.57 was obtained from the AIOD analysis with ANN.

3.4 Stress-strain and void ratio

The average stress-strain relationship of the triplicate CTCS specimens is shown in Fig. 12. The average uniaxial compressive strength (UCS) and the strain of the three specimens were 6.83 MPa and 0.06 respectively. The average void ratio (e) for the tested CTCS specimens was 0.36. An increase in the void ratio increases the area available for fluid flow, thereby increasing the permeability for critical conditions.

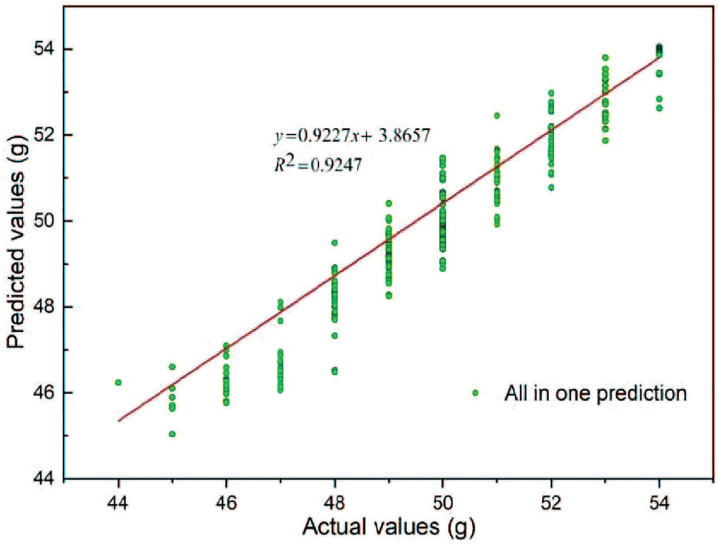

Fig. 10. All-in-one relationship between actual and predicted results

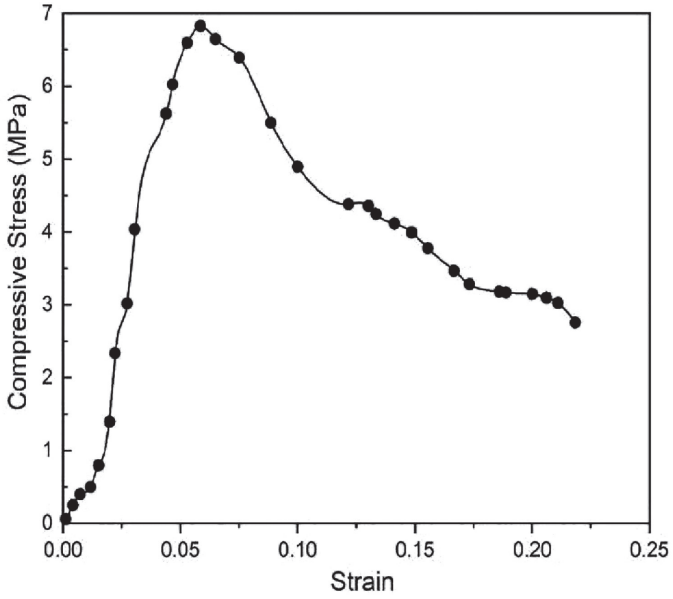

Fig. 11. Stress-Strain relationship for Mindola CTCS

3.5 Arduino load cell creeping with dynamic load

Before starting the hydraulic conductivity testing, the beaker was weighed on an accurate Mini Libra 2000gx0.1 Digital Scale to determine the weight of the empty beaker, which was subsequently used to compare with the final weight in the recorded dataset. It was found that the load cell creeping under dynamic loading was within acceptable limits. Table 2 shows the

Table 2
Load cell creeping for a dynamic load

Sample ID	Mass of empty beaker	Mass of beaker on the standard scale after testing	The final mass of seeped water	Final mass on Arduino Scale	Difference in mass
I	109.4	273.3	163.9	165	1.1
II	109.5	265.7	156.2	154	-2.2
III	109.4	358.9	249.5	250	0.5

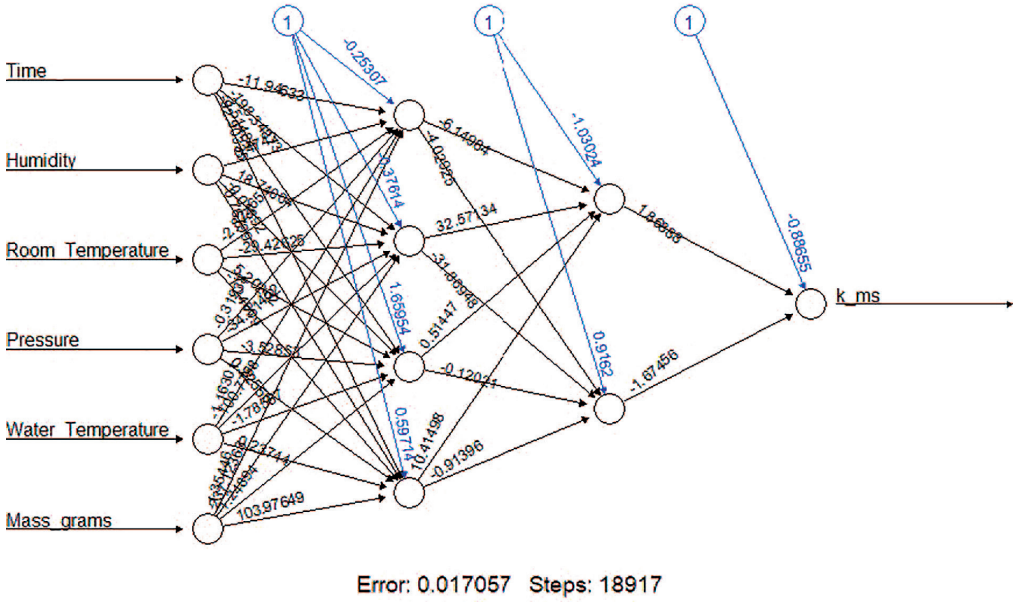

Fig. 12. Artificial neural network for specimen (I)

creep of the Arduino load cell after the permeability test. Table 2 shows that the weight difference between the standard scale and the Arduino scale is consistent with the standard deviation determined for the creep of the load cell under a constant load of 50 g within 24 hours.

3.6 Hydraulic conductivity prediction

An ANN was used to predict the permeability of the tested samples under study by applying the logged dataset. Each dataset was divided into 80% for training and 20% for testing. Fig.s 13, 15, and 17 show the ANN for specimens I, II, and III respectively, while Fig.s 14, 16, and 18 show the coefficient of permeability as a function of duration in seconds for specimens I, II, and III, respectively. Each specimen was tested separately by applying the same confining and seepage pressures. The RMSE of specimen I was $6.24e^{-11}$, predicted mean was $1.55e^{-9}$ and the actual mean was $1.59e^{-9}$; the RMSE, predicted mean, and the actual mean of specimen II were $7.15e^{-11}$, $1.721e^{-9}$ and $1.75e^{-9}$, respectively, while the RMSE, predicted mean and the actual mean for specimen III were $2.0e^{-10}$, $2.26e^{-9,}$ and $2.42e^{-9}$, respectively.

The exponential asymptotic regression models were fitted to the ANN results by iteration in the OriginPro program. In

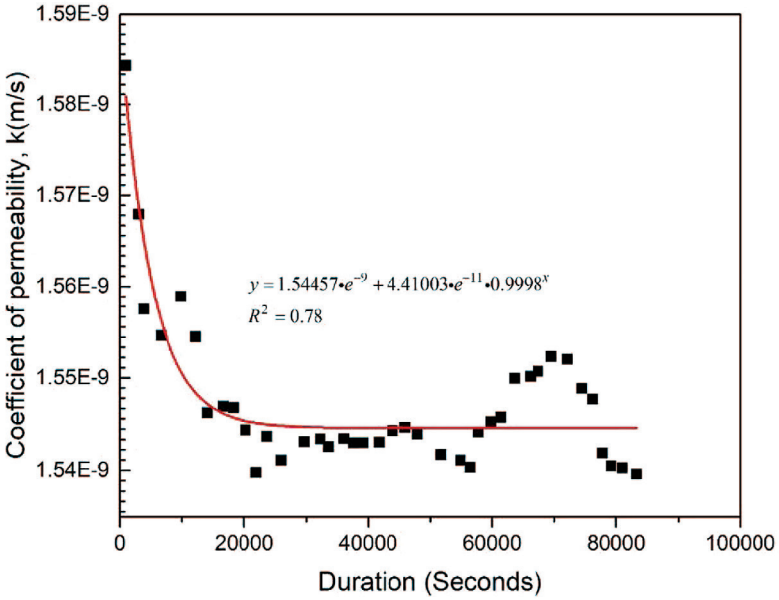

Fig. 13. Hydraulic Conductivity of CTCS specimen (I)

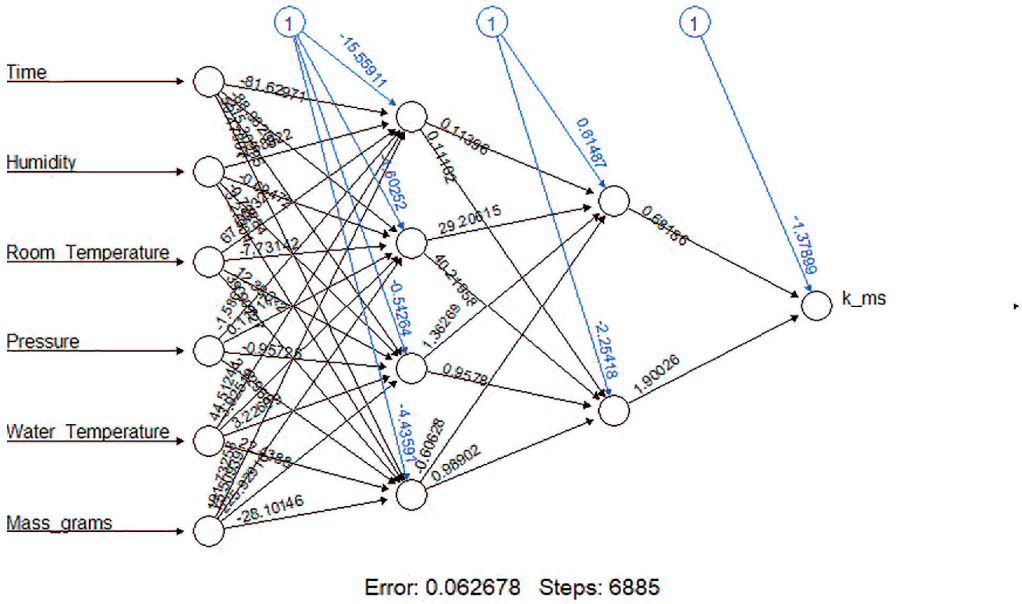

Fig. 14. Artificial neural network for specimen (II)

the case of a non-continuous monitoring permeameter system, it can be deduced that specimen I reached its steady state between 20000–45000 seconds, as shown in Fig. 14. However, due to the change in temperature between 45000–75700 seconds, there was an increment in the coefficient of permeability, because of the change in the

water viscosity, resulting in an increment in the amount of water flowing through the specimen. Fig. 16 shows a typical steady-state condition because the duration of temperature change was shorter than that of specimens I and III. This is because the viscosity of water did not alter the results as shown in Fig. 20. Fig. 20 shows the temperature change during the permeation of the three specimens [4], [34].

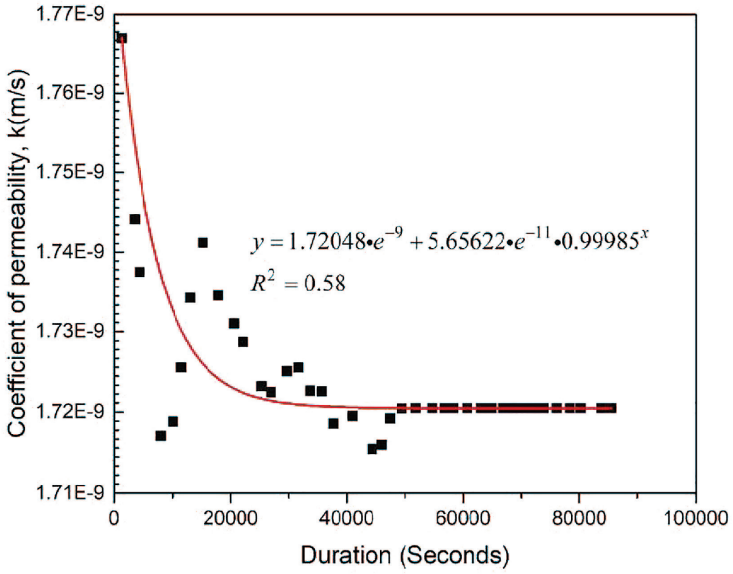

Fig. 15. Hydraulic Conductivity of CTCS specimen (II)

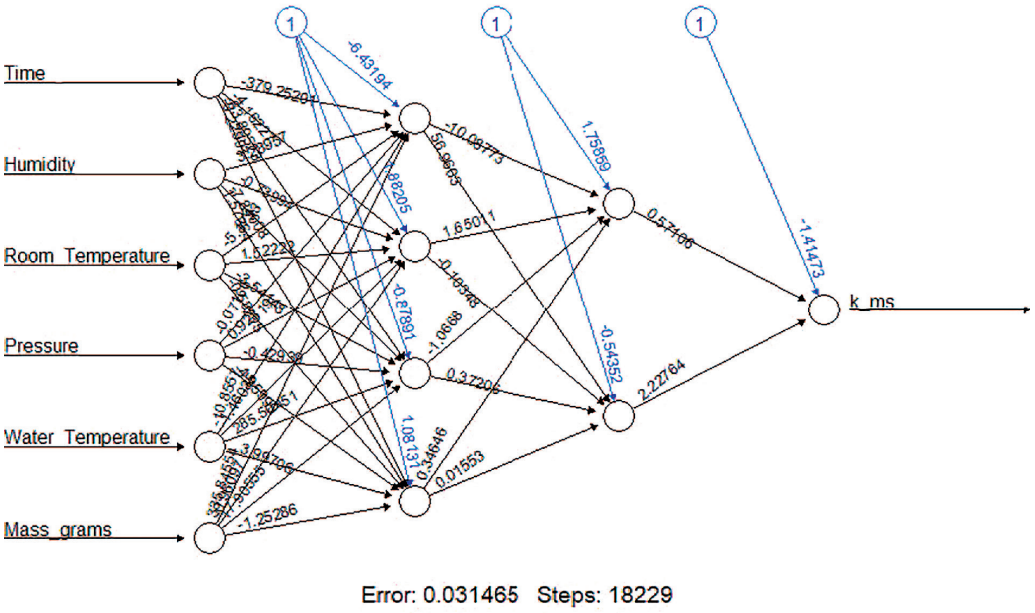

Fig. 16. Artificial neural network for specimen (III)

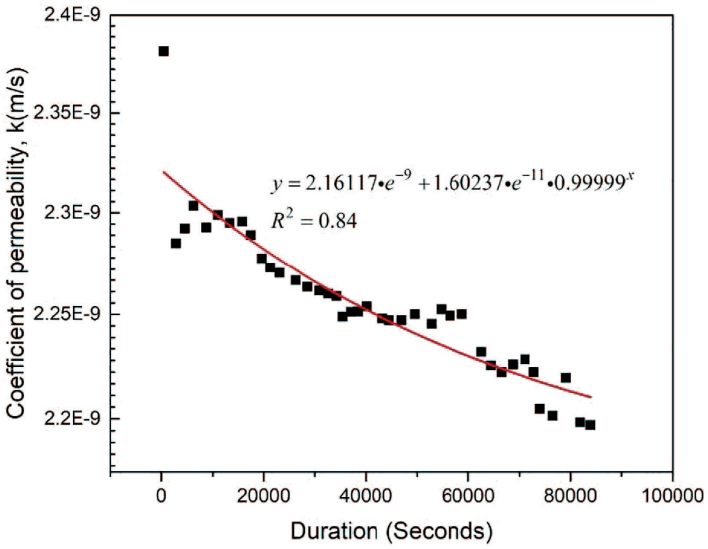

Fig. 17. Hydraulic Conductivity of CTCS specimen (III)

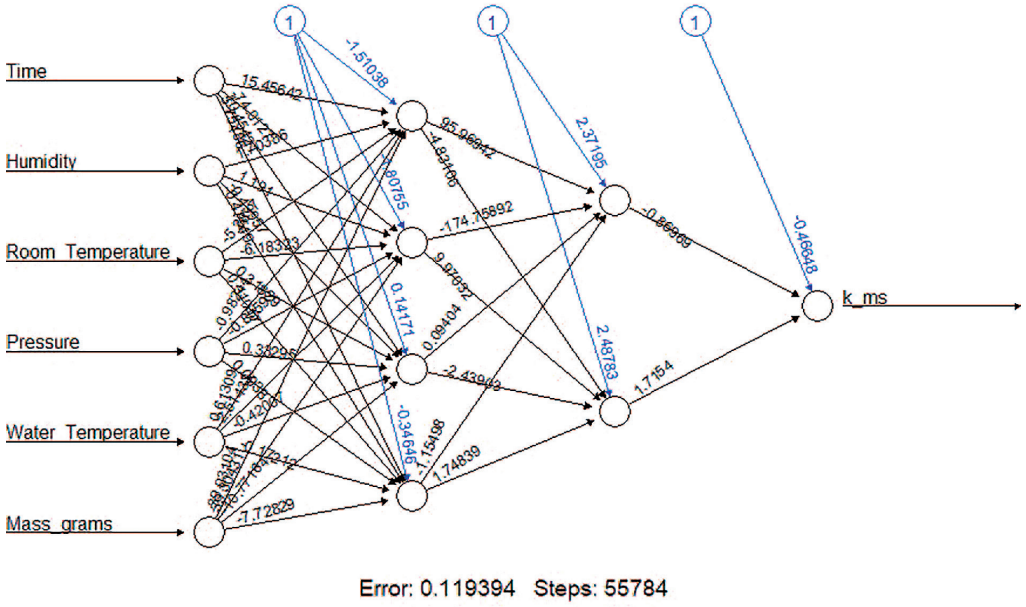

Fig. 18. Artificial neural network for all-in-one actual vs predicted

Finally, the datasets from specimens I, II, and III were combined to predict the all-in-one coefficient of permeability. It was found that the RMSE was $3.10e^{-10}$ m/s, the predicted mean value was $1.73e^{-9}$m/s, and the actual mean value was $1.92e^{-9}$ m/s. Therefore, the coefficient of permeability for the tested CTCS was $1.73e^{-9}$ m/s with a very high coefficient of determination.

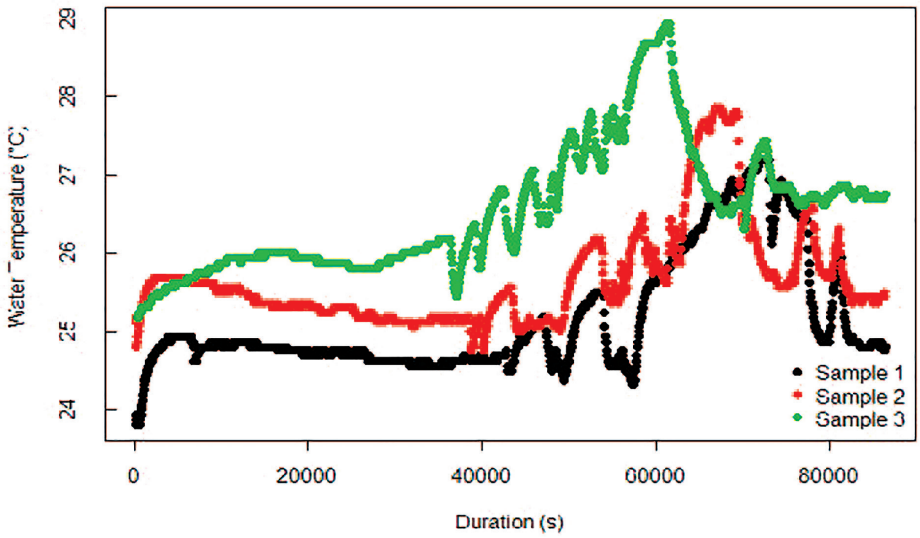

Fig. 19. Temperature change in relation to the duration

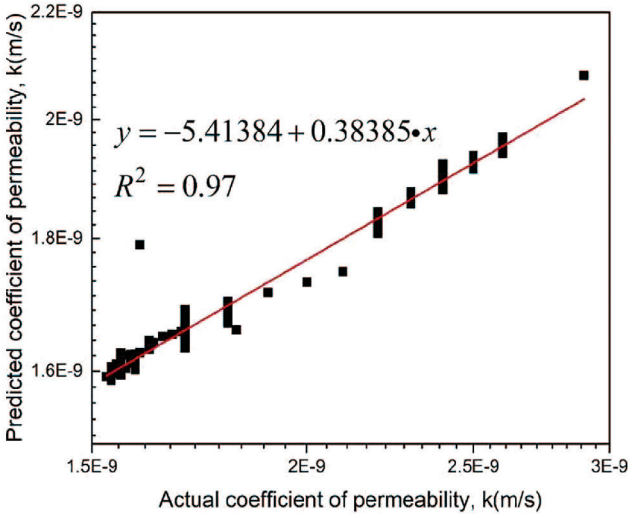

Fig. 20. Relationship between all-in-one actual and predicted

4.0 Conclusions

This study presents the research of possible applications of Arduino sensors and microcontrollers in the fabrication of a one-way triaxial permeameter. Automation of a one-way flexible-wall triaxial permeameter was investigated and implemented at a cost of $2970.

Data acquisition from the one-way triaxial permeameter was automated using Arduino sensors and a microcontroller. The Arduino microcontroller was programmed using Arduino Language, and the data logging application was programmed using Visual Basic Language in the Visual Studio integrated development environment. The

Arduino sensors and the microcontroller were found to be suitable for use in real-time permeameter fabrication.

Environmental factors that affect the creep of the load cell were investigated. Real-time temperature fluctuations were found to be one of the main factors affecting the creep of the load cell. The creep of the load cell over 24 hours was found to be within the acceptable limit for permeability determination. The environmental factor in hydraulic conductivity testing affects not only water viscosity but also pressure regulators.

The stability of using the Arduino load cell to measure the effluent water was investigated using the artificial neural network. Therefore, the Arduino load cell can register a dynamic load like seepage water from the petameter with an accuracy of 0–2.4 g for 24 hours.

The prediction of hydraulic conductivity using machine learning has been found to be an ideal method that can be implemented to accurately predict the hydraulic conductivity of porous materials. Therefore, this methodology can help to determine hydraulic conductivity from the logged data with a high coefficient of determination R2> 0.90.

We would like to express our acknowledgments to Mr. Jack Phiri from AA-Electronics for the technical support, and Dr. Kawawa Banda for providing the flexible pipes to the research group.

REFERENCES

1. Ryan, C. R., Day, S. R. (2002). Soil-cement-bentonite slurry walls. Deep Foundations 2002: An International Perspective on Theory, Design, Construction, and Performance, 116, 713–727.

2. Reid, R. A. (1987). Triaxial Permeability Device. Atlanta: Georgia Institute of Technology.

3. Joshaghani, M., Ghasemi-Fare, O., Ghavami, M. (2018). Experimental investigation on the effects of temperature on physical properties of sandy soils. IFCEE 2018: Installation, Testing, and Analysis of Deep Foundations, 294, 675–685.

4. Ye, W.-M., Wan, M., Chen, B., et al. (2012). Temperature effects on the unsaturated permeability of the densely compacted GMZ01 bentonite under confined conditions. Engineering Geology, 126, 1–7.

5. Head, K. H., Epps, R. J. (2011). Manual of Soil Laboratory Testing. Vol. II. Dunbeath: Whittles Publishing.

6. Siemens, G., Blatz, J. (2007). Development of a hydraulic conductivity apparatus for bentonite soils. Canadian Geotechnical Journal, 44, 997–1005.

7. A dozen ways to measure fluid level. ABB. URL: https://new.abb.com/products/measurement-products/level/a-dozen-ways-to-measure-fluid-level (Access date: 10.02.2022).

8. Wang, S. W., Chen, C. C., Wu, C. M., et al. (2018). A continuous water-level sensor based on the load cell and floating pipe. IEEE International Conference on Applied System Invention (ICASI), 151–154.

9. Buyong L. United States Patent. 19 (2000).

10. Aravind, R., Kumar, A., Harisudhan, K., et al. (2018). Load Cell-based Fuel Level Measurement using Arduino Uno Microcontroller. International Journal of Advance Research and Development, 3(3), 159–164.

11. Mitchell, R. A.,Baker, S. M. (1978). Characterizing the creep response of load Cells. VDI-Berichte, 312, 43–48.

12. Mohamed, M., Hasan, E., Aggag, G. (2009). Study of the creep behavior of load cells. Measurement, 42(7), 1006–1010.

13. Kopczynski, T., Ness, D. (2001). Five factors that can affect your weighing system's accuracy. Powder and bulk engineering, 15, 31–37.

14. Head, K. H. (1998). Manual of Soil Laboratory Testing. Vol. 3. New York: John Wiley & Sons, Inc.

15. Ciaburro, G., Venkateswaran, B. (2017). Neural network with R. Birmingham: Packt Publishing.

16. ASTM-C511–13. Standard Specification for Mixing Rooms, Moist Cabinets, Moist Rooms, and Water. (2015). 23–25.

17. Evans, J., Mclane, M., Conners, S., et al. Development and Calibration of a Lab size Slump Cone. Geo-solutions. URL: https://www.geo-solutions.com/resources/calibration-slump-cone/ (Access date: 25.04.2020).

18. Malusis, M. A., Evans, J. C., Mclane, M. H., et al. (2008). A Miniature Cone for Measuring the Slump of Soil-Bentonite Cutoff Wall Backfill. Geotechnical Testing Journal, 31(5), 373–380.

19. ASTM-D5084–16a. Standard Test Methods for Measurement of Hydraulic Conductivity of Saturated Porous Materials Using a Flexible Wall Permeameter 1. (2016). 10–11.

20. Dafalla, M., Shaker, A., Elkady, T., et al. (2015). Effects of confining pressure and effective stress on hydraulic conductivity of sand-clay mixtures. Arabian Journal of Geosciences, 8, 9993–10001.

21. Luiz T., Morandini C., Leite L. (2015). Characterization and hydraulic conductivity of tropical soils and bentonite mixtures for CCL purposes, Engineering Geology, 196, 251–267.

22. Wang, C., Liu, F. (2014). Analytical Study on Hydraulic Seepage Pressure behind the Tunnel Lining. Physical and Numerical Simulation of Geotechnical Engineering, 17, 57–61.

23. Moayedi H., Mosallanezhad, M., Rashid, A., et al. (2020). A systematic review and meta-analysis of artificial neural network application in geotechnical engineering: theory and applications. Neural Computing and Applications, 32, 495–518.

24. Ranasinghe, R. A., Jaksa, M. B., Kuo, Y. L., et al. (2017). Application of artificial neural networks for predicting the impact of rolling dynamic compaction using dynamic cone penetrometer test results. Journal of Rock Mechanics and Geotechnical Engineering, 9(2), 340–349.

25. Shahin, M. A., Jaksa, M. B., Maier, H. R. (2001). Artificial neural network applications in geotechnical engineering. Australian Geomechanics Journal, 36, 49–62.

26. Shahin, M. A., Jaksa, M. B., Maier, H. R. (2009). Recent Advances and Future Challenges for Artificial Neural Systems in Geotechnical Engineering Applications. Advances in Artificial Neural Systems, 2009, 308239.

27. Chao, Z., Ma, G., Zhang, Y., et al. (2018). The application of artificial neural network in geotechnical engineering. IOP Conference Series Earth and Environmental Science, 189, 022054.

28. Das, S. K. (2013). Artificial Neural Networks in Geotechnical Engineering: Modeling and Application Issues. Metaheuristics in Water, Geotechnical and Transport Engineering, 231–270.

29. Load Cell Amplifier HX711 Breakout Hookup Guide. SparkFun. URL: https://learn.sparkfun.com/tutorials/load-cell-amplifier-hx711-breakout-hookup-guide/all (Access date: 10.02.2022).

30. Visual Basic.Net. Arduino Data Logger with VB Net (Export to Excel) Step by Step. Youtube. URL: https://www.youtube.com/watch?v=EQpflovuJgw (Access date: 10.02.2022).

31. Crawshaw, A. H., Robinson, A. D. (2002). The Calibration of Force Transducers 'On-the-Fly' (NPL Report CMAM). Teddington: National Physical Laboratory.

32. Brice, L., Knott, A., Wilson, A. (2007). Continuous calibration of force transducers. IMEKO 20th TC3, 3rd TC16 and 1st TC22 International Conference "Cultivating metrological knowledge".

33. Bartel, T. W., Yaniv, S. L. (1997). Creep and creep recovery response of load cells tested according to the U. S. and international evaluation procedures. Journal of research of the National Institute of Standards and Technology, 102(3), 349–362.

34. Gao, H., Shao, M. (2015). Effects of temperature changes on soil hydraulic properties. Soil and Tillage Research, 153, 145–154. ГИАБ

ИНФОРМАЦИЯ ОБ АВТОРАХ

Физонга М.[1,2] — аспирант Юго-Восточного университета и преподаватель Университета Замбии, e-mail: fieldmarsheal@gmail.com, ORCID ID: 0000-0002-6261-4126;

Денг Ю.[1] — профессор, заместитель директора департамента подземного строительства, e-mail: noden@seu.edu.cn, ORCID ID: 0000-0002-8223-8711;
Вонг Ф.[1] — профессор, e-mail: feiwang@seu.edu.cn, ORCID ID:0000-0001-7844-5008;
Чикутве Чанда Е. К.[2] — профессор, заведующий кафедрой горного дела, e-mail: emmanuel.chanda@unza.zm, ORCID ID:0000-0002-2102-9342;
Мутамбо В.[2] — старший преподаватель, e-mail: vmutambo@unza.zm,
ORCID ID: 0000-0003-4394-7192;
Бунда Б.[2] — старший преподаватель, декан Горной школы, e-mail: bbesa@unza.zm, ORCID ID: 0000-0001-9133-592X;
Корир Е.[3] — руководитель, e-mail: ekorir@belgraviaservices.com;
Бваля Д.[4] — научный сотрудник, e-mail: danny.bwalya@energiasimples.pt;
Лиюнгу Дж.[5] — преподаватель, e-mail: jliyungu84@gmail.com;
Чипола П.[6] — горный диспетчер, e-mail: chipolapatrick28@gmail.com;
[1] Институт геотехнической инженерии, Школа транспортной инженерии, Юго-Восточный университет, Нанкин, Китай;
[2] Горная школа Замбийского университета, Кампус Грейт-Ист-Роуд, Почтовый ящик 32379, Лусака, Замбия;
[3] Belgravia Services Limited;
[4] Отдел исследований и разработок Simples Energia Lda Rua Aleixo da mota 86, R / C 4150–044 Порту, Португалия;
[5] Инженерная школа Замбийского университета, Кампус Грейт-Ист-Роуд, Почтовый ящик 32379, Лусака, Замбия;
[6] FQM Trident limited, Калумбила, Северо-Запад, Замбия.
Ответственный автор: *Денг Ю.*[1], e-mail: noden@seu.edu.cn.

INFORMATION ABOUT THE AUTHORS

Fisonga M.[1,2], PhD Student at Southeast University and Lecturer at the University of Zambia, e-mail: fieldmarsheal@gmail.com, ORCID ID: 0000-0002-6261-4126;
Deng Y.[1], Professor, Deputy Director of Underground Engineering, Department, e-mail: noden@seu.edu.cn, ORCID ID: 0000-0002-8223-8711;
Wang F.[1], Professor, e-mail: feiwang@seu.edu.cn, ORCID ID:0000-0001-7844-5008;
Chikutwe Chanda E. K.[2], Professor, Head of Mining Department,
e-mail: emmanuel.chanda@unza.zm, ORCID ID:0000-0002-2102-9342;
Mutambo V.[2], Senior Lecturer, e-mail: vmutambo@unza.zm, ORCID ID: 0000-0003-4394-7192;
Bunda B.[2], Senior Lecturer, Dean School of Mines, e-mail: bbesa@unza.zm,
ORCID ID: 0000-0001-9133-592X,
Korir E.[3], Manager, e-mail: ekorir@belgraviaservices.com;
Bwalya D.[4], Researcher, e-mail: danny.bwalya@energiasimples.pt;
Liyungu J.[5], Lecturer, e-mail: jliyungu84@gmail.com;
Chipola P.[6], Mining Dispatcher, e-mail: chipolapatrick28@gmail.com;
[1] Institute of Geotechnical Engineering, School of Transport Engineering, Southeast University, Nanjing, China;
[2] School of Mines, University of Zambia, Great East Road Campus, PO Box 32379, Lusaka, Zambia;
[3] Belgravia Services Limited;
[4] R&D Dept Simples Energia Lda Rua Aleixo da mota 86, R/C 4150–044 Porto, Portugal;
[5] School of Engineering, University of Zambia, Great East Road Campus, P. O. Box 32379, Lusaka, Zambia;
[6] FQM Trident limited, Kalumbila, Northwestern, Zambia.

Получена редакцией 20.03.2022; получена после рецензии 15.07.2022; принята к печати 10.09.2022.
Received by the editors 20.03.2022; received after the review 15.07.2022; accepted for printing 10.09.2022.